Multispectral simulation environment for modeling low-light-level sensor systems

Emmett J. Ientilucci, Scott D. Brown, John R. Schott, and Rolando V. Raqueño

Digital Imaging and Remote Sensing Laboratory
Chester F. Carlson Center for Imaging Science
Rochester Institute of Technology
54 Lomb Memorial Drive
Rochester, NY 14623-5604

ABSTRACT

Image intensifying cameras have been found to be extremely useful in low-light-level (LLL) scenarios including military night vision and civilian rescue operations. These sensors utilize the available visible region photons and an amplification process to produce high contrast imagery. It has been demonstrated that processing techniques can further enhance the quality of this imagery. For example, fusion with matching thermal IR imagery can improve image content when very little visible region contrast is available. To aid in the improvement of current algorithms and the development of new ones, a high fidelity simulation environment capable of producing radiometrically correct multi-band imagery for low-light-level conditions is desired. This paper describes a modeling environment attempting to meet these criteria by addressing the task as two individual components: *(i)* prediction of a low-light-level radiance field from an arbitrary scene, and *(ii)* simulation of the output from a low-light-level sensor for a given radiance field.

The radiance prediction engine utilized in this environment is the Digital Imaging and Remote Sensing Image Generation (DIRSIG) model which is a first principles based multi-spectral synthetic image generation model capable of producing an arbitrary number of bands in the 0.28 to 20 μm region. The DIRSIG model is utilized to produce high spatial and spectral resolution radiance field images. These images are then processed by a user configurable multi-stage low-light-level sensor model that applies the appropriate noise and modulation transfer function (MTF) at each stage in the image processing chain. This includes the ability to reproduce common intensifying sensor artifacts such as saturation and "blooming". Additionally, co-registered imagery in other spectral bands may be simultaneously generated for testing fusion and exploitation algorithms.

This paper discusses specific aspects of the DIRSIG radiance prediction for low-light-level conditions including the incorporation of natural and man-made sources which emphasizes the importance of accurate BRDF. A description of the implementation of each stage in the image processing and capture chain for the LLL model is also presented. Finally, simulated images are presented and qualitatively compared to lab acquired imagery from a commercial system.

Keywords: DIRSIG, image intensifier, low light level (LLL), synthetic image generation, image simulation

1. INTRODUCTION

1.1. Low-Light-Level Imagers

Conventional photo multiplier tubes (PMTs) are able to detect small numbers of photons due to a staged amplification process that converts a single photon into a measurable number of electrons. An adaptation of this technology has resulted in devices that amplify an entire field of photons, allowing us to image under low-light-level (LLL) conditions. This image intensification (II) technology has been available for some time in the form of *night vision goggles* which are frequently used by the reconnaissance community for surveillance and by the Coast Guard to help find shipwreck victims at sea. More recently, these instruments have been evaluated for more domestic applications such as vehicle collision avoidance.

Of specific interest to this research is the design and operation of image intensified charge-coupled devices (IICCDs) which incorporate a micro-channel plate (MCP) for the amplification process, a phosphor screen for electron-to-photon conversion

Part of the SPIE Conference on Image Intensifiers and Applications
San Diego, California • July 1998
SPIE Vol. 3434 • 0277-786X/98/$10.00

and a charge-coupled device (CCD) to capture the intensified image. IICCDs are sensitive in the visible (VIS) region of the electromagnetic (EM) spectrum with some near infrared (near-IR) and ultraviolet (UV) sensitivity. This sensitivity region can provide a reasonable amount of resolution with adequate contrast under moderately low-light-level conditions. However, under extremely low-light-level conditions, these devices can become dominated by noise and there ability to clearly reproduce the imaged scene decreases. In contrast, under high illumination conditions, IICCDs can over-amplify the scene and saturate the CCD resulting in the "blooming" (the apparent spread or overflow of light into neighboring pixels) of bright objects. Some of these effects can be resolved by the use of smart gain control in the intensifier stage. However, even with the utilization of auto gain control (AGC), IICCDs have an small intrascene dynamic range. Under extreme illumination conditions, a more appropriate sensor to use might be a thermal infrared (TIR) sensor which relies on emissive contrast rather than reflective contrast. For example, a TIR sensor can produce high contrast at the horizon due to the typically high thermal contrast between the terrestrial landscape and the cold sky. The disadvantage of the TIR sensor, however, is the lack of spatial resolution when compared to many LLL sensor systems.

1.2. An Application of Image Fusion

More advanced hybrid imaging systems acquire imagery from an intensified imager and TIR imagery simultaneously. By doing so, real-time or post processing techniques can be utilized to fuse the two image products to gain the specific advantages of each sensor types. For instance, the fused image product might utilize the ability of the thermal sensor to resolve the horizon and suppress the effects of "blooming" by the IICCD while still providing the visible cues such as lighting and shadows intuitive to the common observer. Real-time fusion of LLL-VIS/IR image fusion has been performed to generate a hybrid imagery useful for collision avoidance or improved situational awareness.[1]

1.3. Utilizing Synthetic Imagery for Algorithm Development

The rapid increase in computational power has resulted in a significant increase in the ability of developers to more accurately model everything from weather systems to combustion engines. The understanding of the physics and phenomenology needed to generate accurate and realistic looking synthetic images has also improved, and the remote sensing community has benefited from these advances. Synthetic image generation (SIG) can be used as a tool to train image analysts as to the appearance of a target under different meteorological conditions, times of day, or look angles. In addition, SIG can be used to help designers evaluate various sensor systems before the actual hardware is fabricated. Synthetic images can also help determine the optimum acquisition parameters for a real imaging system by predicting the time at which the greatest contrast or visibility will be obtained for the desired targets.

Since synthetic imagery can provide the user with "ground truth" for every pixel in the scene, SIG products have been used most recently in the development and evaluation of image algorithms. For example, landcover classification, spectral unmixing and image fusion algorithms can be evaluated for their ability to correctly reproduce expected results. This results in a potential savings in research and development costs as well as increased performance and operational capabilities. To aid in the evaluation of low-light-level instruments and applications, a high fidelity simulation environment capable of producing radiometrically correct multi-band imagery for low-light-level conditions is desired.

1.4. Motivation

The motivation for this ongoing research is to generate a baseline tool in a synthetic image generation environment for future analysis of IICCD instruments and applications. This includes correctly identifying and including image formation parameters critical in low-light-level radiance field predictions. Additionally, a tool is currently under development for the simulation of a generic IICCD systems including the inclusion of optical MTF effects, photon distribution statistics, intensifier effects and artifacts, and system noise contributions. With these tools in place, the ability to model new instruments and systems will allow hardware designers and algorithm developers to experiment with new ideas without the cost of a complex development process.

2. BACKGROUND

2.1. The DIRSIG Model

Originally, The Digital Imaging and Remote Sensing (DIRS) laboratory's Image Generation (DIRSIG) model was designed as a longwave infrared (LWIR) sensor model aimed at simple two dimensional target-to-background calculations for IR signature studies. It evolved to a full 3-D thermal IR image generation model with an imbedded thermal model for target and background temperature estimation. In the 1980's, solar reflection terms were added and the model's spectral range was extended from the long wave infrared (LWIR) down into the visible. Today DIRSIG incorporates spectral texture treatments, transmissive objects, and plume modeling.

The DIRSIG model generates scene images using a rigorous radiometric prediction of target signatures that utilizes surface BRDF to predict surface reflected radiances based on the incident radiance from the hemisphere above the target [2] and spectrally applied surface textures.[3] MODTRAN is utilized to compute path dependent transmission, scattering, emission and downwelling radiances.[4] Additional reflective region components include natural illumination sources (sun, moon) and man-made sources (lights, etc.). In the thermal region, temperature predictions are produced by THERM, a passive slab thermal model that incorporates thermodynamic attributes, 24-hours of weather, pixel-by-pixel sun-shadow history and sky exposure factors.[5]

DIRSIG can produce simulated imagery from both framing array sensors and scanning focal planes (line-scanners, push-broom scanners, etc.) at a user defined spatial resolution. The output image can be either integrated radiances from multi-spectral systems (discrete bands) and hyper-spectral imaging spectrometers (continuous adjacent bands), or spectral radiances at a user defined spectral resolution (possibly for post-simulation application of a suite of sensor responses).

The usefulness of these synthetic images is negated if the output does not closely imitate the real world.[6] As a result, the output from SIG must be evaluated and assessed according to criteria such as spectral and radiometric accuracy, geometric fidelity, robustness of application, and speed of image generation. The relative importance of these parameters, however, will vary depending on the use of the SIG imagery. In this research we will concern ourselves with preserving radiometric and geometric fidelity as well as replicating common artifacts from intensifying sensors such as localized blooming.

2.1.1. Reflective Region Modeling

For the shorter wavelength region of the spectrum dominated by reflectance terms, the exoatmospheric solar and lunar sources dominate the source of reflected photons (depending on the time of day). DIRSIG utilizes ephemeris data to determine the location and state (i.e., phase of the moon, etc.) of both the solar and lunar bodies for the requested simulation time. This information is passed to MODTRAN to compute the direct irradiance from both of these extraterrestrial sources at the mean target location. This allows the model to predict target illumination radiances for any time including the difficult dawn and dusk periods. The ephemeris data is also used by the thermal to predict the solar insulation history for any point in the scene.

In addition to the primary extraterrestrial sources, the model also incorporates the full sky hemisphere illumination into the reflected radiance terms. For day light periods, this hemispherical sky map is computed by repeated calls to MODTRAN to determine the scattered radiance from a series of locations in the sky. For nighttime simulations, atmospheric scattering from the lunar source is not as significant, however, starlight can be an important contributor in new moon and near new moon scenarios. In these cases, the spectral starlight term comes from published data on the irradiance of the night-sky which specifies the whole sky radiance (rather than a hemispherical map).[7] Example imagery from a DIRSIG night simulation that incorporates lunar and man-made illumination sources appears in Figure 1. The simulated man-made sources are high-intensity incandescent lights, however, spectral exitance curves for any source can be input (for example, sodium or mercury vapor lamps).

Surface reflected radiances are computed using a hemispherical sampling method for determining the incident radiance from portions of the hemisphere above the surface, including the radiance from adjacent objects, the sky and active exoatmospheric sources. Each spectral radiance sample of the hemisphere is then modified by the geometry specific reflectance (from the material's bi-directional reflectance distribution function), weighted by the solid area of the sample, and added to the total reflected radiance. The hemisphere is sampled at a higher resolution in the specular direction so that the blurring effects of a non-zero area specular lobe are reproduced in the generated imagery. This approach reproduces both the shape of specular reflections and the effects of spectral bleeding from adjacent objects observed in diffuse surfaces.

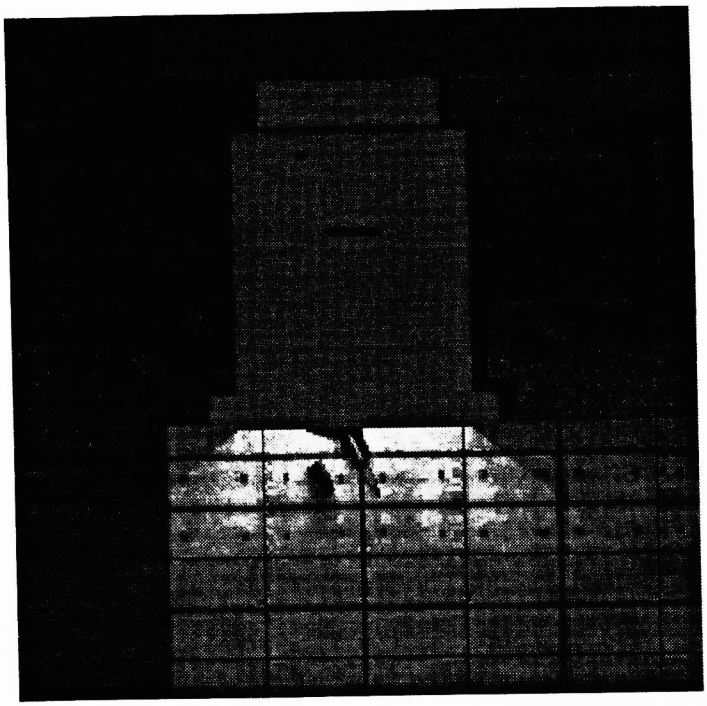

Figure 1. A DIRSIG broadband visible region simulation of an airfield at night under half-moon conditions. Lights inside the hangar illuminate the parking area outside the hangar.

2.2. Low-Light-Level Systems

Image intensifiers amplify the available photons contained in and around the scene of interest. Most image intensifiers contain a photocathode surface, which is irradiated by the focused image field by a front-end optical system. The photocathode absorbs incident light and converts it to photoelectrons, forming a low-energy photoelectron image. This photoelectron image is then accelerated to several kilovolts by the a potential difference between the photocathode and the phosphor screen located at the rear of the intensifier. The accelerated photoelectrons then impact the fluorescent screen consisting of P20 or RCA-10-52 designate phosphor, which converts the photoelectron image back to visible photons.[8] Since the phosphor screen can emit several hundred photons when impacted by a photoelectron having 10 to 20 keV energy, an overall net gain in the number of photons results.

The research completed to date has focused on image intensified CCDs (IICCDs) (or simply intensified CCDs (ICCDs)). These image intensifying instruments are used in industrial and scientific applications and mate a conventional image intensifying device to a CCD. Commonly, these instruments utilize a microchannel plate (MCP) or microchannel plate stack with a phosphor screen on the outside, which is optically coupled to a CCD array (see Figure 2). The scene is imaged onto the photocathode, and an intensified copy then is produced on the phosphor, which the CCD records. These detectors are similar to the photon counting cameras in that the quantum efficiency is limited by the photocathode material. The intensifier, however, is not limited to incident radiation in the visible part of the EM spectrum. For example, the photocathode can be made sensitive to X-rays, ultraviolet (UV), or infrared (IR) radiation. In this context, the intensifier performs a means of image conversion.

CCD read noise is not generally a problem with ICCD instruments because the image recorded has been significantly amplified. The ideal photo-counting device gives a δ function response to a detected photon event, in both space and time. With ICCDs, individual photons are not recorded as δ functions, but are the images of phosphor flashes, which can spread over several pixels and may last more than one frame, depending on the phosphor decay time.[9]

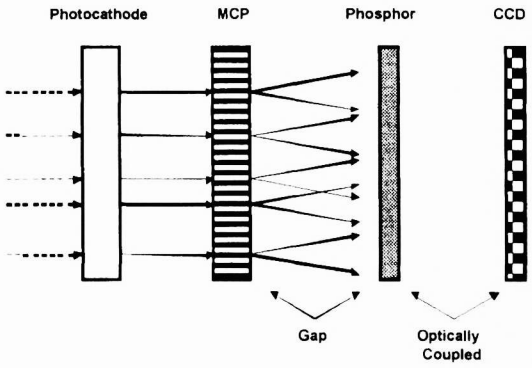

Figure 2 Basic schematic of an intensified CCD instrument.

3. SYSTEM MODELING: A CHAIN APPROACH

The overall approach to synthetic modeling is illustrated in Figure 3. The DIRSIG input parameters include the scene database (objects in scene, thermodynamic and reflectances databases, etc.), the atmospheric databases (path transmissions, scattered radiances, meteorological data) and information on exoatmospheric and man-made sources. The result is a high fidelity radiance field image which is processed by the low-light-level sensor simulator. The sensor simulation is broken down into the physical elements of a generalized IICCD. Each simulation element reflects a different stage in the processing of the input radiance field. The variability of photon arrival in a low-intensity image is modeled with the appropriate distribution and then passed to the optics model. The optics model currently only introduces image wide MTF effects due to the entrance aperture, however, geometric effects due to non-uniformity in the optics could be modeled. The image intensifier is modeled as a gain stage with an additional MTF due to the spread of exiting photons by the phosphor. In high intensity or gain scenarios, the imaging CCD may become saturated and "blooming" may occur. Finally, the image is processed by any additional MTF and noise effects introduced by the back-end electronics (such as amplifier noise, quantization and MTF from video converters, etc.).

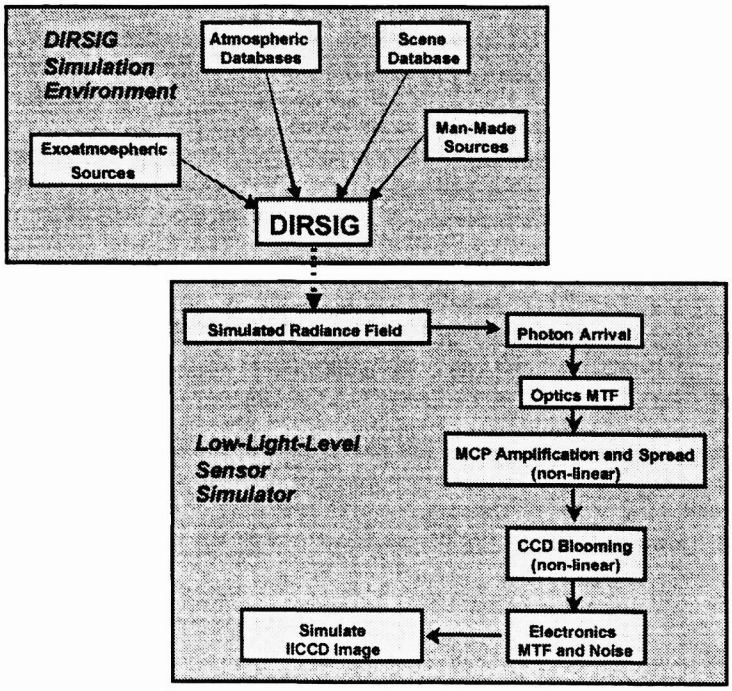

Figure 3. The DIRSIG based low-light-level imagery simulation environment.

3.1. Case Study: PULNiX IICCD

To demonstrate the current capabilities of this simulation environment, simulations of a commercial system were performed for qualitative comparison to the actual system. The instrument of interest is an image intensified CCD (IICCD), Generation III device with a GaAs photocathode. The characterization parameters came from the AG-5745EF-3 automatic gated intensified CCD manufactured by PULNiX America Inc. Tables 1.1 and 1.2 shows the cameras specifications.

Table 1.1 **Intensifier Tube Specifications.**

Type	18mm gated, proximity focus
Input	1in (18mm diameter)
Output	2/3in (tapered-fiber coupled to CCD)
Photocathode	GaAs
Phosphor Screen	P20
Gain	15,000 (typical)
Resolution	64 lp/mm
Distortion	N/A
EBI	3.5×10^{-11} lm/cm^2
Spectral resolution	500 nm - 925 nm
Magnification	1

Table 1.2 **CCD Camera Specifications.**

Imager	2/3in interline transfer CCD
Pixel	768 (H) x 493 (V)
Cell size	11 μm × 13 μm
Scanning	525 lines 60 Hz, 2:1 interlace
TV resolution	570 (H) × 359 (V)
S/N ratio	50 dB min.
Min Illumination	0.5 lux f-1.4 without IR cut filter
Video output	1.0 Vpp composite video, 75Ω
AGC	ON
Gamma	1.0
Tube Life	Est. 20,000 hrs.

3.1.1. Lab Collected Imagery

For this preliminary demonstration, a simple lab collection was performed using the PULNiX camera. The imaged target consisted of a four-bar target and an approximate point source. A series of images were acquired under a variety of room illuminations. A sample image from the collected data set in Figure 4 displays some of the artifacts common to imagery from IICCD instruments including the blooming of the point source in the upper right corner and observable image wide noise.

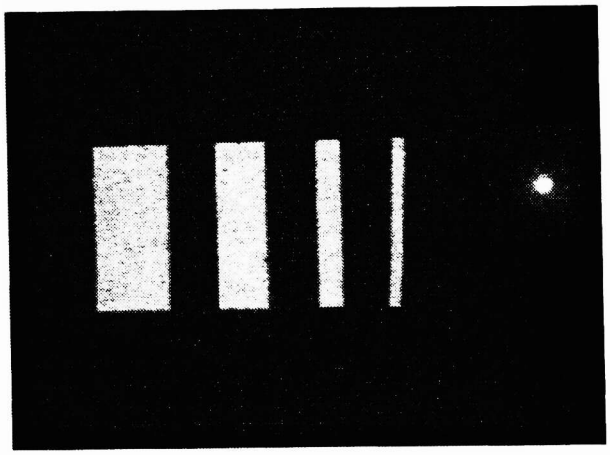

Figure 4. Actual image of the lab target acquired with the PULNiX camera. The bright spot in the upper right corner is a point source.

In addition to these images, a series of experiments were performed to gain an operational knowledge of the sensor noise as a function of illumination and gain, the spatial extend of blooming under controlled gain scenarios, and system MTF (including video conversion). More precise characterizations can be acquired from product literature, previously investigated and published results, or in-house measurements using published techniques.[10, 11, 12] Published studies range from resolution testing on gated intensifiers [13] to improved photocathode designs.[14-15] For these preliminary experiments, however, only a qualitative estimation of the system's performance characteristics was used.

3.1.2. Simulated Imagery

In order to simulate the lab collected imagery, the radiance field image shown in Figure 5 was hand made to match auxiliary measurements made in the lab. Note that the point source has a significant area which reflects the illumination by the point

source of the thin film and holder around the pinhole. This image was then placed into the IICCD processing chain using the parameterized values for the sensor.

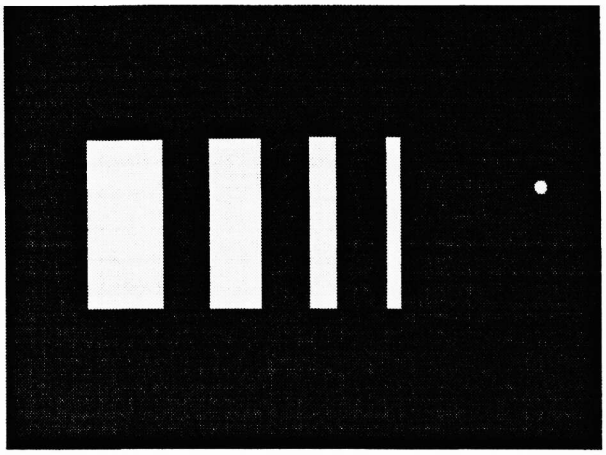

Figure 5. Hand-generated radiance field imaged used in preliminary testing of LLL sensor simulator. Point source area reflects illumination of holder ring.

The resulting processed image in Figure 6 features many of the first order effects observed in the lab collected imagery. For instance, the saturation and blooming of the point source indicate that the appropriate models for this phenomenon have been correctly identified and implemented. A rigorous statistical study of the image wide noise has not been conducted at this time but will be part of future validation efforts.

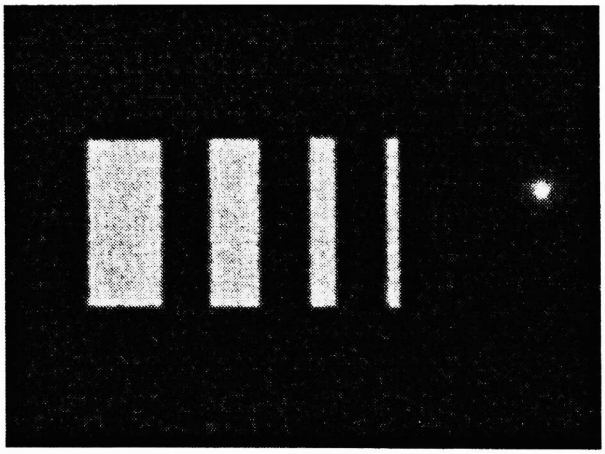

Figure 6. Simulated IICCD output using lab measured characteristics of the IICCD camera used in this experiment.

4. APPLICATION TO VIS/IR IMAGE FUSION

4.1. Fusion introduction

The goal for VIS/IR sensor fusion is to provide a composite image that can be easily and intuitively exploited to rapidly extract the relevant information contained in both of the independent acquisitions of the scene. A common application for low-light VIS/IR sensor fusion is to improve situational awareness for use in night driving aids.[16] A group at MIT's Lincoln Labs has been performing real time image fusion with this in mind. Their work involves the real time (low latency) fusion of low-light visible and thermal IR imagery by combining the sensor's complementary information into a single color video stream for display to the user. Although this technique can significantly improve the interpretability of the imagery, the governing radiometry for the process is simplified and more elaborate techniques might be devised using physically based algorithm that produce even better hybrid imagery. Or perhaps, alternative bands (other than the visible or thermal IR regions) might be utilized for other applications (i.e. monitoring plant stress or water quality).

4.2. Fusion of DIRSIG Simulated Imagery

To demonstrate of the use of this synthetic environment for end-to-end modeling, DIRSIG was used to generate a low-light VIS and thermal IR pair for use in a simplified fusion algorithm (see Figure 7). The modeled scene is an airfield and hangar including a fighter aircraft and support vehicle. The simulated acquisition time was 0200 hours local time under clear sky, new moon conditions. Lighting was added inside the aircraft hangar to provide a source of photons for the low-light-level camera to be modeled (left image). The IR image has the image wide spatial contrast we expect from the thermal region of the spectrum (right). Additionally, note the colder surfaces on the tops of the vehicle and aircraft that are exposed to the cold clear sky.

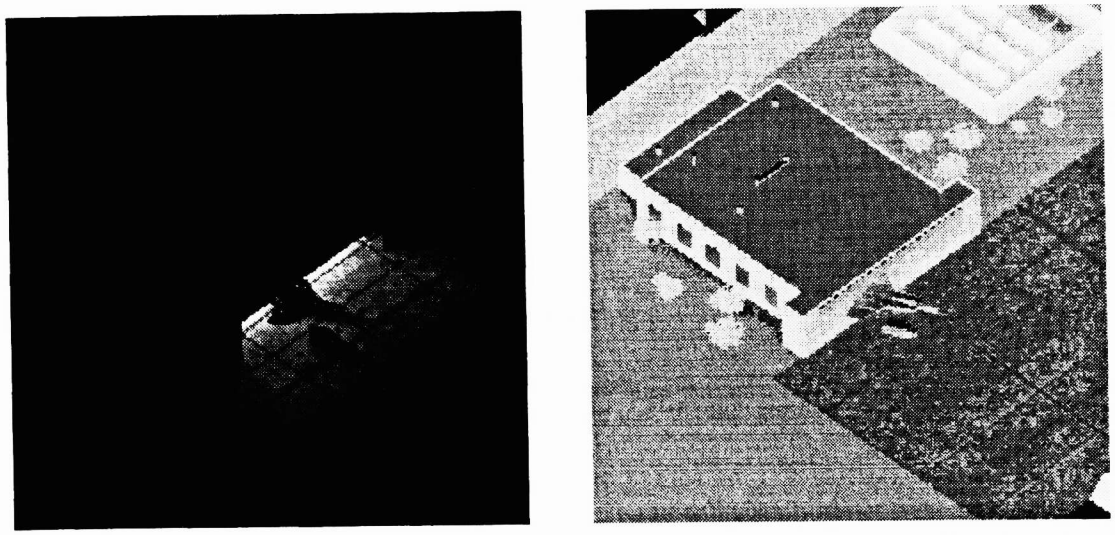

Figure 7. DIRSIG simulated visible (left) and thermal IR (right) radiance fields of an airfield hangar. Simulation time is 0200 hours under new moon conditions.

The visible radiance filed image was processed using the preliminary characterization of our PULNiX camera and a user specified gain. The thermal IR image was also processed using noise and MTF characteristics of an Inframetrics scanning IR imager. These two images where then fused using a simple weighted addition to produce the imagery in Figure 8. Some blooming of the IICCD sensor can be observed along the edge of the hangar.

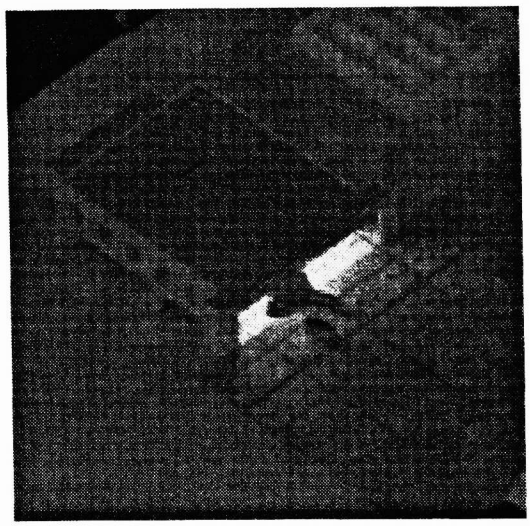

Figure 8. Fused product of the DIRSIG simulated images. Low-Light-Level sensor image used had all currently modeled artifacts included.

4.3. Using SIG for Fusion Algorithm Development

The use of synthetic imagery for algorithm development allows the engineer to evaluate the effects of changes in acquisition parameters and conditions without the cost associated with a rigorous collection. In addition, the developer gains the availability of more accurate truth data than is conventionally available with field collect data. In regards to the development of better fusion products, the engineer can easily experiment with the use of alternate bands in the fusion process, different sensor responses (spectral shape), the possibility of multi-band fusion, new feedback and gain controls for the low-light-level camera, and approaches to compensate for the effects of blooming.

5. CONCLUSIONS

Additions to the DIRSIG model have been made to improve the radiometric accuracy and realism for low-light-level imaging conditions including the incorporation of the moon as an additional exoatmospheric source, star light and man-made sources. A simulation environment for low-light-level sensors has also been created and continues to be developed that allows the user to model a variety of IIT and IICCD instruments. At this time, only crude lab characterizations of our in-house sensor have been demonstrated, however, the use of more rigorous characterizations is desired and will be attempted in the future.

This effort has demonstrated how SIG can be used to simulate the output from fusion algorithms. Future efforts should focus on methods to compensate for extreme CCD blooming from staring at sources or viewing specular glints. For example, using information from the compliment image should be investigated as well as multi-band fusion and noise suppression techniques.

REFERENCES

1 Waxman, A.M., Savoye, E.D. Gay, D.A., Aguilar, M., Gove, A.N., Carrick, J.E., Racamato, J.P., "Electronic imaging aids for night driving: low-light CCD, uncooled thermal IR, and color-fused visible/LWIR," *Proc. SPIE*, vol. 2902, p.62-73, (1997).

2 Brown, S.D., Schott, J.R., Raqueno, R.., "Incorporation of bi-directional reflectance characteristics into the Digital Imaging and Remote Sensing Image Generation Model", *Proceedings of the Ground Target Modeling and Validation Conference*, (1997).

3 Schott, J.R., Salvaggio, C., Brown, S.D, Rose, R.A., "Incorporation of texture in multispectral synthetic image generation tools", *Proceedings of the SPIE Aerosense Conference,* Targets and Backgrounds: Characterization and Representation, Vol. 2469, No. 23, (1995).

4 Berk, A., Bernstein, L.S., Robertson, D.C., "MODTRAN: a moderate resolution model for LOWTRAN 7," GL-TR-89-0122, Spectral Sciences, Burlington, MA, (1989).

5 DCS Corporation, "AIRSIM thermal signature prediction and analysis tool model assumptions and analytical foundations", DCS Technical Note 9090-002-001, (1991).

6 Brown, S.D., Schott, J.R., Raqueno, R., Kraska, T., White, R., "Validation of the Digital Imaging and Remote Sensing Image Generation Model, DIRSIG", *Proceedings of the Ground Target Modeling and Validation Conference*, (1996).

7 RCA Electro-Optics Handbook, RCA Corporation, Commercial Engineering, Harrison, NJ, 07029, (1974).

8 Csorba, Illes P., "Image intensifiers in low light level and high speed imaging," *SPIE Milestone Series*, vol. MS20, p.113-118, (1986).

9 Horch, E., "Speckle imaging in astronomy," *International Journal of Imaging Systems and Technology*, vol. 6, p.401-417, (1995).

10 Flynt, William E., "Measurement of modulation transfer function in image tubes: effects of spurious background brightness," *Proc. SPIE*, vol. 1952, p.276-280, (1993).

11 Gagne, Robert M., West, Charles N., Wagner, Robert F., Quinn, P.W., "Laboratory measurements of sensitometry, MTF, veiling glare, Wiener spectrum and DQE for image intensifier tubes," *Proc. SPIE*, vol. 1896, p.248-258, (1993).

12 Lapington, Jonathan S., "Investigation of image non-linearity's in a photon counting image tube," *Proc. SPIE*, vol. 2209, p.549-556, (1994).

13 Thomas, Matthew C., Yates, George J., Zagarino, Paul A., "Resolution and shutter profile measurements with point source inputs for a microchannel-plate image intensifier (MCPII) with a 160-ps FWHM whole-image shutter," *Proc. SPIE*, vol. 2551, p.181-188, (1995).

14 Sinor, Timothy W., Estrea, Joseph P., Phillips, David L., Rector, M. K., "Extended blue GaAs image intensifiers", *Proc. SPIE*, vol. 2551, p.130-134, (1995).

15 Estrea, Joseph P., Sinor, Timothy W., Passmore, Keith T., Rector, M. K., "Development of extended red (1.0- to 1.3-um) image intensifiers," *Proc. SPIE*, vol. 2551, p.135-144, (1995).

16 Toet, A., Ijspeert, J.K., Waxman, A.M., Aguilar, M., "Fusion of visible and thermal imagery improves situational awareness," *Proc. SPIE*, vol. 3088, p. 177-188, (1997).